

Gap Nodes and Time Reversal Symmetry Breaking in Strontium Ruthenate

James F. Annett and B. L. Gyor'y

H. H. Wills Physics Laboratory, University of Bristol, Tyndall Ave, BS8-1TL, UK.

G. Litak

Department of Mechanics, Technical University of Lublin,
Nadbystrzycka 36, 20-618 Lublin, Poland.

K. I. Wysokiński

Institute of Physics, M. Curie-Skłodowska University,
Radziszewskiego 10, 20-031 Lublin, Poland

(Dated: January 10, 2022)

We study the superconducting state of Sr_2RuO_4 on the bases of a phenomenological but orbital specific description of the electron-electron attraction and a realistic quantitative account of the electronic structure in the normal state. We found that a simple model which features both 'in plane' and 'out of plane' coupling with strengths $U_k = 40\text{ meV}$ and $U_\gamma = 48\text{ meV}$ respectively reproduced the experimentally observed power law behaviour of the low temperature specific heat $C_v(T)$, superfluid density $n_s(T)$ and thermal conductivity in quantitative detail. Moreover, it predicts that the quasi-particle spectrum on the γ -sheet is fully gaped and the corresponding order parameter breaks the time reversal symmetry. We have also investigated the stability of this model to inclusion of further interaction constants in particular between orbitals contributing to the γ -sheet of the Fermi surface and the δ and ϵ sheets. We found that the predictions of the model are robust under such changes. Finally, we have incorporated a description of weak disorder into the model and explored some of its consequences. For example we demonstrated that the disorder has a more significant effect on the f-wave component of the order parameter than on the p-wave one.

I. INTRODUCTION

The symmetry of the order parameter in superconducting Sr_2RuO_4 has been a subject of intense experimental and theoretical interest in recent years^{1,2}. It is probably the best candidate, currently, for an odd-parity, spin triplet, superconductor which would be a charged particle analogue of superfluid ^3He .³ Although a number of other superconductors are also possible spin-triplet superconductors (including UPt_3 , UGe_2 , ZrZn_2 , and Bedgaard salts) strontium ruthenate is probably the one which is best characterized experimentally. Samples can be grown which have exceptionally long mean free paths,⁴ and above T_c the normal state is a Fermi liquid with a well understood Fermi surface⁵.

Currently controversy exists over two key aspects of the Sr_2RuO_4 pairing state. Firstly, the gap function symmetry is still not known. Rice and Sigrist⁶ suggested several possible gap functions for Sr_2RuO_4 corresponding to analogues of superfluid phases of ^3He . Of these only the analogue of the Anderson-Brinkman-Morel (ABM) state³,

$$d(\mathbf{k}) = (k_x + ik_y)\hat{e}_z; \quad (1)$$

is consistent with the observations of a constant γ -plane Knight shift⁷ and spin susceptibility⁸ below T_c . This state is also consistent with the γ -SR experiments which show spontaneous time reversal symmetry breaking at T_c .¹² However this gap function has no zeros on the three cylindrical Fermi surface sheets⁵ of Sr_2RuO_4 , in direct contradiction to several experiments which in-

dicate that the gap function has lines of zeros on the Fermi surface^{9,10,11}. This discrepancy is not easily resolved since a complete group theoretic classification of all symmetry distinct pairing states in tetragonal crystals^{13,14,15,16,17,18} do not include any states which have both spontaneous time reversal symmetry breaking at T_c and symmetry required line nodes on a cylindrical Fermi surface.¹⁷ A number of 'f-wave' gap functions have been proposed^{19,20,21} for Sr_2RuO_4 ,

$$d(\mathbf{k}) = f(\mathbf{k})\hat{e}_z; \quad (2)$$

where $f(\mathbf{k})$ is an $l = 3$ spherical Harmonic function. Such gap functions have constant γ -plane Knight shift and may have both time reversal symmetry breaking and line nodes, however in tetragonal symmetry crystals they are always either of fixed symmetry (requiring a double phase transition) or are in the same symmetry class (E_u) as $l = 1$ 'p-wave' states which do not have line nodes. Such f-wave functions may be possible physically (depending on the details of the actual pairing interaction), but the line nodes are not required by the symmetry of the pairing state.

The second controversy about the Sr_2RuO_4 gap function concerns the presence of three different Fermi surface sheets, γ , δ , and ϵ . The orbital dependent superconductivity model of Agterberg, Sigrist and Rice²⁴ envisioned a dominant gap on one part the Fermi surface (originally δ), with the gap function on the other band only arising from interband coupling and hence being significantly smaller. This theory predicted that weak impurity scattering would destroy the small gap on the inactive sheet,

and hence lead to a finite residual density of states at zero energy. However the experimental specific heat data⁹ shows that $C_V \propto T$ is zero at $T = 0$, and hence there is a finite order parameter on all sheets of the Fermi surface. In a recent letter, Zhitomirsky and Rice²⁵ have argued that the gap function of superconducting strontium ruthenate can be described by an effective, k -space, interband-proximity effect. In this model they propose that the superconductivity is due to an attractive interaction in the p -wave channel, which is acting almost entirely on one sheet of the Fermi surface, the δ sheet. The other two Fermi surface sheets, α and β , are driven to become superconducting because of a "proximity effect" or Josephson like coupling between the α and β bands. This model has a number of features which are consistent with the experimental facts, such as the presence of both line-nodes in the gap function and spontaneous time reversal symmetry breaking below T_c . Furthermore, if the interband Josephson coupling energy is chosen to be sufficiently large, then the energy gap at low temperatures is moderately large on all the Fermi surface sheets and there is no second peak below T_c in the specific heat capacity.

In a recent paper we have proposed a quite general semi-phenomenological methodology for studying the possible superconducting states of Sr_2RuO_4 . In this approach one chooses, more or less systematically, orbital and position dependent interaction constants to describe the electron-electron attraction. The simplest useful model we have studied prominently featured inter-layer coupling²⁶. This model characterizes the pairing interaction in terms of two nearest-neighbor negative- U Hubbard interactions, one, U_k acts between $\text{Ru } d_{xy}$ in a single RuO_2 plane, while the second, U_γ acts between $\text{Ru } d_{xz} d_{yz}$ orbitals between planes. When these two parameters are chosen so as to give a single phase transition temperature at the observed T_c of 1.5K we find excellent agreement with the measured specific heat, penetration depth and thermal conductivity data. The gap function has both time reversal symmetry breaking, but also horizontal lines of nodes in the planes $k_z = \pm c$ on the Fermi surface sheet. The δ sheet remains node-less, with a gap function of the form $d(k) = (\sin k_x + i \sin k_y) e_z$, corresponding to the 2-d analogue of the $^3\text{He A}$ -phase. The predicted gap function is similar to that of Zhitomirsky and Rice (ZR)²⁵, but differs in that it is more or less same size on all three Fermi surface sheets. Moreover, while ZR rely on 'proximity coupling' to avoid the double phase transition we exploit the freedom provided by the experimental data and achieve the same end by fixing both U_k and U_γ so that there is only one transition at the observed $T_c = 1.5\text{K}$.

The purpose of this paper is to clarify a number of unresolved questions concerning the interlayer coupling model. Firstly we show in Section III that the results of the model are quite generic, and do not depend sensitively on the choice of the specific Hubbard model parameters which we used in Ref.²⁶. Secondly we examine

the effects of weak disorder on the gap function (Section IV). We show that weak disorder can suppress any f -wave components of the gap function, while leaving the p -wave order parameter relatively unchanged. Finally in Section V we study the generalisation of our model by allowing for a "bond proximity" interactions. Such symmetry mixing interactions have been proposed by Zhitomirsky and Rice²⁵ as a mechanism leading to the single superconducting transition temperature. It turns out that the mechanism operates in the orbital picture as well and we obtained the single superconducting transition temperature, but different slope and jump of the specific heat.

II. GAP SYMMETRY AND PAIRING BASIS FUNCTIONS

Let us begin by reviewing briefly the symmetry principles which are used to classify different pairing symmetry states in odd-parity superconductors. We shall use these principles to contrast the different pairing states that have been proposed for strontium ruthenate.

On very general ground we expect that the phase transition into the superconducting state is of second order, and so there exists an order parameter, or set of order parameters, $\phi_i(\mathbf{r}); i = 1; \dots; n$. For superconductors these order parameters are complex, transforming under the $U(1)$ gauge symmetry as $\phi_i \rightarrow e^{i\theta} \phi_i$. Therefore the Ginzburg-Landau Free energy can always be expanded as

$$F_s = F_n + \int d^3r \left[\frac{\hbar^2}{2m} \partial_{ijk} \phi_i(\mathbf{r}) \partial_{kjl} \phi_j(\mathbf{r}) + \sum_{ijkl} a_{ijkl} \phi_i(\mathbf{r}) \phi_j(\mathbf{r}) \phi_k(\mathbf{r}) \phi_l(\mathbf{r}) + \dots \right] \quad (3)$$

where summation convention is implied for the indices i, j etc, and as usual $\partial_i = \nabla_i - 2e i A_i / \hbar$, with A the magnetic vector potential.

If the normal state above T_c possesses a symmetry group G , then the order parameters ϕ_i can be grouped into terms corresponding to the different irreducible representations of G , transforming under symmetry operations as

$$\phi_i \rightarrow R_{ij}(g) \phi_j \quad (4)$$

where $g \in G$, and the matrices $R_{ij}(g)$ constitute the representation of the group G .

The general theory of group representations implies that we can choose a basis in which the matrix R_{ij} is block diagonal, with each block corresponding to an irreducible representation, Γ . In this basis the full Ginzburg-Landau Free energy is of the form

$$F_s = F_n + \int d^3r \left[\frac{\hbar^2}{2m} \partial_{ijk} \phi_i(\mathbf{r}) \partial_{kjl} \phi_j(\mathbf{r}) + \sum_{ijkl} a_{ijkl} \phi_i(\mathbf{r}) \phi_j(\mathbf{r}) \phi_k(\mathbf{r}) \phi_l(\mathbf{r}) + \dots \right] \quad (5)$$

TABLE I: Irreducible representations of even and odd parity in a tetragonal crystal. The symbols X, Y, Z represent any functions transforming as x, y and z under crystal point group operations, while I represents any function which is invariant under all point group symmetries.

Rep.	symmetry	Rep.	symmetry
A_{1g}	I	A_{1u}	$XYZ(X^2 - Y^2)$
A_{2g}	$XY(X^2 - Y^2)$	A_{2u}	Z
B_{1g}	$X^2 - Y^2$	B_{1u}	XYZ
B_{2g}	XY	B_{2u}	$Z(X^2 - Y^2)$
E_g	$fXZ; YZg$	E_u	$fX; Yg$

TABLE II: Products of the irreducible representations of D_{4h} point group symmetry

	A_1	A_2	B_1	B_2	E
A_1	A_1	A_2	B_1	B_2	E
A_2	A_2	A_1	B_2	B_1	E
B_1	B_1	B_2	A_1	A_2	E
B_2	B_2	B_1	A_2	A_1	E
E	E	E	E	E	A_1, A_2, B_1, B_2

$$\begin{aligned}
& + \sum_{ij} X_{ij} \phi_i(\mathbf{r}) \phi_j(\mathbf{r}) \\
& + \sum_{ijkl} X_{ijkl} \phi_i^0(\mathbf{r}) \phi_j^0(\mathbf{r}) \phi_k^0(\mathbf{r}) \phi_l^0(\mathbf{r}) :
\end{aligned} \quad (5)$$

The quadratic term $\sum_{ij} X_{ij} \phi_i \phi_j$ involves only a single representation, A_{1g} . At T_c , in general, only a single irreducible representation will have a zero eigenvalue of the block diagonal matrix X_{ij} . Therefore only the components of the order parameter ϕ_i corresponding to that eigenvector will become non-zero just below T_c .

Now let us apply these very general principles to the specific case of spin-triplet pairing in Sr_2RuO_4 . This is a body-centred tetragonal crystal with inversion symmetry. The relevant crystal group is D_{4h} , and Table I shows its irreducible representations. For each representation its symmetry is denoted by a typical function, where the symbols X, Y, Z represent any functions which transform as x, y and z under the point group operations, and I means any function which is invariant under all point group operations. The representations $A_{1g} \dots E_g$ have even parity, while $A_{1u} \dots E_u$ have odd parity. Table II shows the multiplication table for the irreducible representations, i.e. how direct products of representation matrices $\Gamma_i \Gamma_j$ decompose into a sum of block diagonal matrices $\Gamma_1 \Gamma_2 \dots$.

An immediate consequence of the multiplication table II is that in tetragonal crystals the order parameter is either of a single representation only, or there are two or more distinct thermodynamic phase transitions. This is because to quadratic (or higher) order in the Ginzburg-Landau free energy there are no symmetry allowed cou-

TABLE III: Basis functions $\phi_i(\mathbf{k})$ for the odd parity irreducible representations of body-centred tetragonal crystals.

Rep.	in-plane	inter-plane
A_{1u}	—	—
A_{2u}	—	$\cos \frac{k_x}{2} \cos \frac{k_y}{2} \sin \frac{k_z c}{2}$
B_{1u}	—	$\sin \frac{k_x}{2} \sin \frac{k_y}{2} \sin \frac{k_z c}{2}$
B_{2u}	—	—
E_u	$\sin k_x$ $\sin k_y$	$\sin \frac{k_x}{2} \cos \frac{k_y}{2} \cos \frac{k_z c}{2}$ $\cos \frac{k_x}{2} \sin \frac{k_y}{2} \cos \frac{k_z c}{2}$

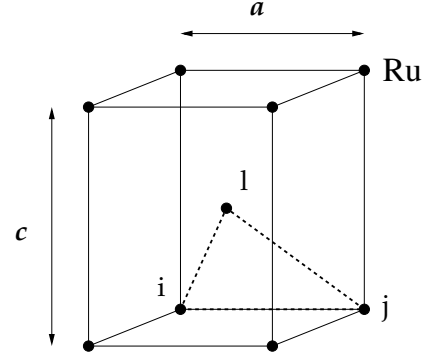


FIG. 1: Body-centred tetragonal lattice, showing the nearest neighbour pairs in-plane, and between planes.

pling terms of the form

$$\sum_{ijkl} X_{ijkl} \phi_i^0(\mathbf{r}) \phi_j^0(\mathbf{r}) \phi_k^0(\mathbf{r}) \phi_l^0(\mathbf{r})$$

in Eq. 5. The proof⁷ is simply that A_{1g} never contains the identity representation A_{1g} , and hence such terms are not allowed as quartic invariants of the Free energy (or at higher order). In the absence of such terms the free energy functional is always of at least quadratic order in the subdominant order parameter $\phi_i(\mathbf{r})$, and hence these subdominant components can only become non-zero in a separate phase transition below T_c .

Using these irreducible representations we can expand the BCS gap function in terms of functions of each separate symmetry class. For odd parity pairing states we can represent the BCS gap function by a vector $\mathbf{d}(\mathbf{k})$ or a symmetric 2×2 complex matrix

$$\begin{pmatrix} d_{yy}(\mathbf{k}) & d_{yz}(\mathbf{k}) \\ d_{yz}(\mathbf{k}) & d_{xx}(\mathbf{k}) + id_{xy}(\mathbf{k}) \end{pmatrix} = \begin{pmatrix} d_y(\mathbf{k}) & d_z(\mathbf{k}) \\ d_z(\mathbf{k}) & d_x(\mathbf{k}) + id_y(\mathbf{k}) \end{pmatrix} \quad (6)$$

where $d_{xx}(\mathbf{k}) = d_{xx}(\mathbf{k})$ and $d_{yy}(\mathbf{k}) = d_{yy}(\mathbf{k})$. For each irreducible representation we can choose a complete set of orthonormal basis functions in the Brillouin zone, $\phi_i(\mathbf{k})$. Expanding the gap function in terms of these functions we have

$$\mathbf{d}(\mathbf{k}) = \sum_i \mathbf{d}_i \phi_i(\mathbf{k}) \quad (7)$$

The expansion coefficients essentially provide the set of order parameters in Eq. 5. The basis functions must be

periodic in reciprocal space, $\psi_i(\mathbf{k}) = \psi_i(\mathbf{k} + \mathbf{G})$, or equivalently, they must obey periodic boundary conditions in the 1st Brillouin zone. They can be chosen, most naturally, in terms of their real-space Fourier transforms, which correspond to lattice sums of the real-space Bravais lattice. For a body-centred tetragonal crystal, such as Sr_2RuO_4 shown in Fig. 1, the leading basis functions correspond to the four nearest-neighbour in-plane lattice vectors, $\mathbf{R} = a\hat{\mathbf{e}}_x$ and $\mathbf{R} = a\hat{\mathbf{e}}_y$, giving two odd-parity basis functions: $\sin k_x a$ and $\sin k_y a$. The eight body-centred lattice vectors $\mathbf{R} = \frac{a}{2}\hat{\mathbf{e}}_x - \frac{a}{2}\hat{\mathbf{e}}_y - \frac{c}{2}\hat{\mathbf{e}}_z$ lead to the four odd-parity basis functions shown in the last column of Table III (where for simplicity we have chosen units of length such that $a = 1$). In the models which we investigate in the remainder of this paper, we shall assume that these basis functions, Table III, are sufficient to describe the gap function. Physically this corresponds to the assumption that the pairing interaction $V_0(\mathbf{r}; \mathbf{r}^0)$ is short ranged in real-space.

Considering Table I we can see that in Sr_2RuO_4 "p-wave" pairing states can correspond to either the A_{2u} , (or p_z) representation or the doubly degenerate E_u representation (p_x, p_y). The only symmetry distinct "f-wave" pairing states are the B_{1u} and B_{2u} representations, corresponding to f_{xyz} and $f_{(x^2 - y^2)z}$ type symmetries. Neither of these states can be used in the case of a two-dimensional single-plane model of Sr_2RuO_4 , since they both become zero in the plane $k_z = 0$. It is also interesting to note that in Table III there are no basis functions of A_{1u} or B_{2u} symmetry. Pairing in these channels would require long range interactions extending to at least the inter-plane second nearest neighbors.

In the light of these symmetry principles let us comment on a number of the possible gap functions which have been proposed for Sr_2RuO_4 . Among the few states described by Rice and Sigrist⁶ the only one consistent with the Knight shift experiments is¹⁷

$$d(\mathbf{k}) = (\sin k_x + i \sin k_y) \hat{\mathbf{e}}_z \quad (8)$$

belonging to the E_u representation of Table III. It breaks time reversal symmetry, consistent with the $-SR$ experiments of Luke et al.¹², and leads to a spin susceptibility which is constant below T_c for fields in the ab plane, consistent with Knight shift⁷ and neutron scattering experiments⁸. However it has no gap nodes on a Fermi surface of cylindrical topology, such as the α , β and γ sheets of Sr_2RuO_4 , and therefore is inconsistent with the heat capacity⁹ penetration depth¹⁰ and thermal conductivity experiments¹¹.

On the other hand the f-wave gap function proposed by Won and Maki²⁰

$$d(\mathbf{k}) = k_z (k_x - i k_y)^2 \hat{\mathbf{e}}_z \quad (9)$$

has both line nodes and broken time reversal symmetry below T_c . However from the symmetry analysis above, it is clear that this does not correspond to a single irreducible representation of the symmetry group. It is a sum

of the function $k_z (k_x^2 - k_y^2)$, belonging to B_{2u} and $k_x k_y k_z$ belonging to B_{1u} . Although they would be degenerate in a system with cylindrical symmetry, in a tetragonal crystal they will be non-degenerate and hence have different T_c s. The B_{1u}, B_{2u} states individually possess time reversal symmetry. Therefore with this order parameter we would expect to find a specific heat anomaly with two transitions, and time reversal symmetry breaking would only occur at temperatures below the lower transition.

The f-wave order parameter proposed by Graf and Balatsky¹⁹,

$$d(\mathbf{k}) = k_x k_y (k_x + i k_y) \hat{\mathbf{e}}_z \quad (10)$$

is in the same symmetry class as E_u , since $B_2 \otimes E = E$ in Table II. Therefore in the sense of pure symmetry arguments the gap nodes in planes $k_x = 0$ and $k_y = 0$ are "accidental". Such a gap function is certainly valid, but the nodes are present for reasons connected with the specific microscopic pairing interaction employed, and not required by symmetry alone. This comment also applies to the $B_{1u} \otimes E$ f-wave state

$$d(\mathbf{k}) = (k_x^2 - k_y^2) (k_x + i k_y) \hat{\mathbf{e}}_z \quad (11)$$

discussed by Dahm, Won and Maki,²¹ and Eremenko et al.^{22,23}.

The full group theoretic classification in tetragonal crystals^{13,14,15,16,17,18} and the above analysis does not show a single pairing state with both symmetry required lines of nodes and spontaneously broken time reversal symmetry below T_c . Therefore, if we accept both the $-SR$ and low temperature thermodynamic and transport measurements, then we must consider states which have lines of nodes for specific microscopic reasons, rather than for pure symmetry reasons.

In the remainder of this paper we shall focus on the specific model which we proposed in a previous paper²⁶, in which the lines of nodes appear in the plane $k_z = \pm c$, derived from the pair of inter-plane basis functions of E_u :

$$\sin \frac{k_x}{2} \cos \frac{k_y}{2} \cos \frac{k_z c}{2}; \quad \cos \frac{k_x}{2} \sin \frac{k_y}{2} \cos \frac{k_z c}{2}$$

from Table III, as originally suggested by Hasegawa et al.²⁷.

III. INTERLAYER COUPLING HAMILTONIAN

Since the underlying microscopic mechanism for superconductivity in Sr_2RuO_4 is not known we choose to adopt a phenomenological approach to the pairing mechanism. We first make an accurate tight binding fit to the experimentally determined Fermi surface^{5,28} and then introduce model attractive interactions between the different orbitals centered on different sites. We can investigate different 'scenarios' depending upon which model interactions are assumed to dominate. Frequently, when

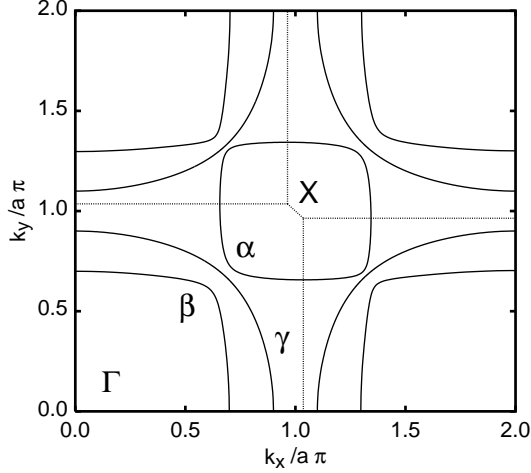


FIG. 2: The Fermi surface of Sr_2RuO_4 in the plane $k_z = 0$, obtained by fitting the de Hass data of Bergman et al.⁵. Note that the alpha Fermi surface sheet has only two-fold symmetry, because of the shape of the Brillouin zone boundary.

these pairing interaction parameters are chosen to reproduce the experimental T_c , there is no freedom to adjust the parameters further. Once the parameters have been selected, then a number of different experimental quantities can be calculated independently and compared to experiment. The goal is to find one specific pairing scenario which agrees with all of the experimental observations. If this can be achieved then one has found an effective Hamiltonian for the pairing, which can be interpreted physically. This effective pairing Hamiltonian can then be used to guide the search for the true microscopic Hamiltonian. This methodology has proved very useful in cuprate superconductivity²⁹ and here we shall deploy it to study Sr_2RuO_4 .

The effective pairing Hamiltonian we consider is a simple multi-band attractive U Hubbard model:

$$\hat{H} = \sum_{i,j,m,m^0} (t_{m,m^0}^{ij}) \hat{c}_{im}^\dagger \hat{c}_{jm^0} + \frac{1}{2} \sum_{i,j,m,m^0} U_{m,m^0}^{ij} \hat{n}_{im} \hat{n}_{jm^0} \quad (12)$$

where m and m^0 refer to the three Ruthenium t_{2g} orbitals $a = xz, b = yz$ and $c = xy$ and i and j label the sites of a body centered tetragonal lattice.

The hopping integrals t_{m,m^0}^{ij} and site energies ϵ_m were fitted to reproduce the experimentally determined Fermi surface^{5,28}. The nearest neighbour in-plane hopping integrals along $\mathbf{R} = \hat{e}_x$, where the ab plane lattice constant is taken to be 1, are constrained by the orbital

symmetry to have the following form

$$[t_{m,m^0}^{ij}] = \begin{pmatrix} 0 & t_{ax} & 0 & 0 \\ 0 & 0 & t_{bx} & 0 \\ 0 & 0 & 0 & t \end{pmatrix} \quad (13)$$

(and similarly for $\mathbf{R} = \hat{e}_y$ taking into account sign changes due to orbital symmetries). The next nearest neighbour in-plane hopping integrals along $\hat{e}_x + \hat{e}_y$ were assumed to be of the form

$$[t_{m,m^0}^{ij}] = \begin{pmatrix} 0 & t_{ab} & 0 \\ t_{ab} & 0 & 0 \\ 0 & 0 & t^0 \end{pmatrix} \quad (14)$$

The parameter t^0 controls the shape of the γ -band Fermi surface, while the parameter t_{ab} determines the hybridization between the a and b orbitals and hence the shape of the β and γ Fermi surfaces. The c -axis magnetic field de Hass van Alphen data²⁸ gives the areas and cyclotron masses of the three Fermi surface sheets, and these six numbers can be fitted exactly with $t = 0.08162\text{eV}$, $t^0 = 0.45t$, $t_{ax} = 1.34t$, $t_{bx} = 0.06t_{ax}$, $t_{ab} = 0.08t_{ax}$, and the on-site energies were $\epsilon_c = 1.615t$ and $\epsilon_a = \epsilon_b = 1.062t_{ax}$.

To obtain a three dimensional Fermi surface we assumed that the dominant inter-plane hopping is along the body-centre vector $\mathbf{R} = \frac{1}{2}(\hat{e}_x + \hat{e}_y + \hat{e}_z)$ and has the form

$$[t_{m,m^0}^{ij}] = \begin{pmatrix} 0 & t_z & t_{hyb} & t_{hyb} \\ t_{hyb} & t_z & t_{hyb} & t_{hyb} \\ t_{hyb} & t_{hyb} & 0 & 0 \end{pmatrix} \quad (15)$$

and similarly for $\mathbf{R} = \frac{1}{2}(\hat{e}_x - \hat{e}_y + \hat{e}_z)$ with appropriate sign changes. The parameter t_{hyb} is the only term in the Hamiltonian which mixes the c orbitals with a and b . With only these two parameters it is not possible to fit exactly the full three dimensional Fermi surface cylinder corrugations determined by Bergman et al.⁵, but the parameters $t_{hyb} = 0.12t_{ab}$, $t_z = 0.03t_{ab}$ give a reasonable agreement for the dominant experimental corrugations. Fig. 2 shows the fitted Fermi surface in the plane $k_z = 0$ in the extended zone scheme. Note that the α sheet has only two-fold symmetry, due to its position centred on the Brillouin zone boundary at X .

The set of interaction constants U_{m,m^0}^{ij} describe attraction between electrons on nearest neighbour sites with spins \uparrow and \downarrow and in orbitals m and m^0 . Thus our actual calculations consists of solving, self-consistently, the following Bogoliubov-de Gennes equation:

$$\begin{pmatrix} E & H_{m,m^0}^{ij} \\ H_{m^0,m}^{ij} & E + H_{m,m^0}^{ij} \end{pmatrix} \begin{pmatrix} u_{jm^0} \\ v_{jm^0} \end{pmatrix} = 0; \quad (16)$$

where H_{m,m^0}^{ij} is the normal spin independent part of the Hamiltonian, and the $u_{jm^0}^{ij}$ is self consistently given in terms of the pairing amplitude, or order parameter, Δ_{m,m^0}^{ij} ,

$$\Delta_{m,m^0}^{ij} = U_{m,m^0}^{ij} \Delta_{m^0,m}^{ij}; \quad (17)$$

defined by the usual relation

$$U_{mm^0}(ij) = \sum_{\mathbf{X}} U_{im} v_{jm^0}(1 - 2f(E_{\mathbf{X}})); \quad (18)$$

where $\sum_{\mathbf{X}}$ enumerates the solutions of Eq.16.

We solved the above system of Bogoliubov de Gennes equations including all three bands and the three dimensional tight-binding Fermi surface. We considered a large number of different scenarios for the interaction constants. First we assumed that the pairing interaction $U_{mm^0}(ij)$ for nearest neighbours in plane is only acting for the c (d_{xy}) Ru orbitals. In this case both a d-wave ($d_{x^2-y^2}$) pairing state and p-wave ($(k_x + ik_y)\hat{e}_z$) states are possible. The d-wave state has line nodes, but would not be consistent with the experiments showing constant Knight shift and time reversal symmetry breaking below T_c . Therefore we discard such solutions here, and only concentrate on the odd-parity spin triplet solutions. The motivation is not to explain the microscopic pairing mechanism, but to model pairing state produced by various types of effective attractive interactions. These attractive interactions may arise from, for instance, ferromagnetic spin fluctuations^{6,22,23,30}, which can favour spin triplet pairing compared to the d-wave solutions. However, their origin may be more complicated, for example a combined electron-phonon and spin fluctuation mechanism.

With only the nearest neighbor in-plane interactions the set of possible odd-parity, spin triplet, solutions that we found never includes any possible state with nodes of the gap. Therefore we extended the model to include inter-plane interactions. Using two interactions, a nearest neighbor in-plane interaction, ($i-j$ in Fig.1), and a nearest neighbor inter-plane interaction, ($i-l$ in Fig.1) which fulfil the tetragonal symmetry, we have the two types of basis functions for the gap equation given in Table III. Then we have the possibility of horizontal line nodes in the gap arising from the zeros of $\cos(k_z c/2)$ at $k_z = \pm c$ on a cylindrical Fermi surface²⁷.

Because the pairing interactions $U_{mm^0}(ij)$ were assumed to act only for nearest neighbor sites in or out of plane, the pairing potential $U_{mm^0}(ij)$ is also restricted to nearest neighbors. We further focus on only odd parity (spin triplet) pairing states for which the vector $\mathbf{d} = (0;0;d^z)$, i.e. $U_{mm^0}^{\#}(ij) = U_{mm^0}^{\#}(ij)$, and $U_{mm^0}^{\#}(ij) = U_{mm^0}^{\#}(ij) = 0$. Therefore in general we have the following non-zero order parameters (i) for in plane bonds: $U_{mm^0}^k(\hat{e}_x)$, $U_{mm^0}^k(\hat{e}_y)$, and (ii) for inter-plane bonds: $U_{mm^0}^{\#}(R_{ij})$ for $R_{ij} = (a=2; a=2; c=2)$.

Taking the lattice Fourier transform of Eq.17 the corresponding pairing potentials in k -space have the general form (suppressing the spin indices for clarity):

$$U_{mm^0}(\mathbf{k}) = U_{mm^0}^{kp_x} \sin k_x + U_{mm^0}^{kp_y} \sin k_y + U_{mm^0}^{\#p_x} \sin \frac{k_x}{2} \cos \frac{k_y}{2} \cos \frac{k_z c}{2} + U_{mm^0}^{\#p_y} \sin \frac{k_y}{2} \cos \frac{k_x}{2} \cos \frac{k_z c}{2}$$

$$+ U_{mm^0}^{\#p_z} \sin \frac{k_z c}{2} \cos \frac{k_x}{2} \cos \frac{k_y}{2} + U_{mm^0}^{\#f} \sin \frac{k_x}{2} \sin \frac{k_y}{2} \sin \frac{k_z c}{2} :: \quad (19)$$

Note that beyond the usual p-wave symmetry of the $\sin k_x$ and $\sin k_y$ type for the c orbitals, we include all three additional p-wave symmetries of the $\sin k=2$ type which are induced by the effective attractive interactions between carriers on the neighboring out-of-plane Ru orbitals. These interactions are also responsible for the f-wave symmetry order parameters, $U_{mm^0}^{\#f}$, transforming as B_{1u} in Table 1. This latter is symmetry distinct from all p-wave order parameters in a tetragonal crystal, unlike the other f-wave states discussed in the introduction^{19,20,21,22}. The p_z order parameters are of A_{2u} symmetry. In contrast the pairs $U_{mm^0}^{\#p_x}$; $U_{mm^0}^{\#p_y}$ are of the same E_u 'p-wave' symmetry as $U_{mm^0}^{kp_x}$; $U_{mm^0}^{kp_y}$. In general, the order parameters in each distinct irreducible representations have different transition temperatures, as expected from Eq. 5.

In a recent paper²⁶ we chose a particularly simple set of attractive pairing interactions $U_{mm^0}(ij)$. For in-plane nearest neighbours we assumed that the pairing interaction is only acting for the c (d_{xy}) Ru orbitals only

$$U_{km^0} = \begin{pmatrix} 0 & 1 \\ 0 & 0 & 0 \\ 0 & 0 & 0 \end{pmatrix} A; \text{ where } U_k = 0.494t; \quad (20)$$

On the other hand, given that the ruthenium a and b orbitals (d_{xz} ; d_{yz}) are oriented perpendicularly to the planes we choose to introduce the inter-plane interaction only for these orbitals,

$$U_{\#mm^0} = \begin{pmatrix} 0 & 1 \\ U_{\#} & U_{\#} & 0 \\ 0 & 0 & 0 \end{pmatrix} A; \text{ where } U_{\#} = 0.590t; \quad (21)$$

Therefore we have, as a minimal set, only two coupling constants U_k and $U_{\#}$ describing these two physically different interactions.

As discussed earlier our strategy is to adjust these phenomenological parameters in order to obtain one transition at the experimentally determined T_c . Thus, beyond fitting T_c , there are no further adjustable parameters, and one can compare directly the calculated physical properties of the superconducting states to those experimentally observed. Consequently, if one obtains a good overall agreement one can say that one has empirically determined the form of the pairing interaction in a physically transparent manner. Evidently such conclusion is the principle aim of the calculations.

As we have shown in Ref26, this two parameter scenario gives an excellent agreement with the experimental specific heat⁹, superfluid density¹⁰ and thermal conductivity¹¹. We chose the constants U_k and $U_{\#}$, so that there is a single phase transition at $T_c = 1.5K$, corresponding to the values given in Eqs.20 and 21. Below T_c

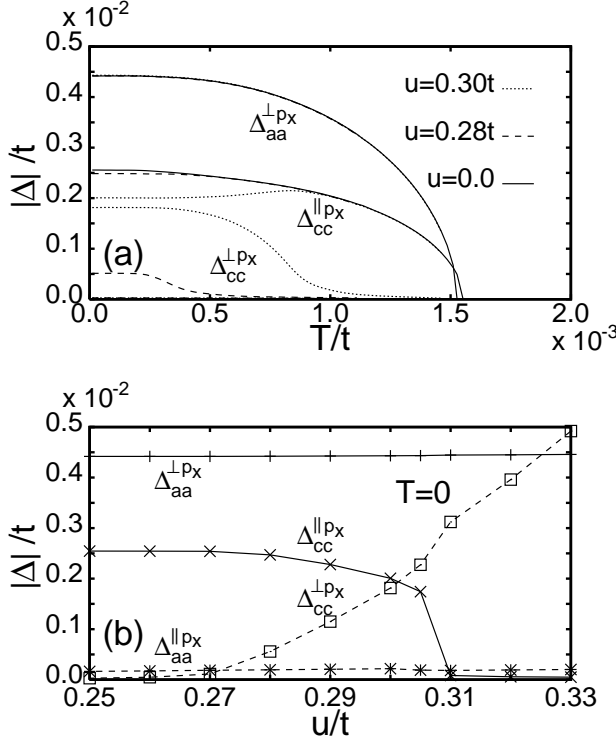


FIG. 3: (a) Temperature dependence of order parameters $j_{aa}^{\perp p_x}$, $j_{cc}^{\perp p_x}$ and $j_{cc}^{\parallel p_x}$ for a number of u values ($u^0 = u$). (b) Order parameters $j_{cc}^{\perp p_x}$ and $j_{aa}^{\perp p_x}$, $j_{cc}^{\parallel p_x}$ at zero temperature versus the interaction parameter u ($= u^0$).

the order parameters have the symmetries $k_{py} = i \frac{k_{px}}{cc}$, $j_{bb}^{\perp p_y} = i \frac{j_{aa}^{\perp p_x}}{aa}$ as expected for an E_u pairing symmetry²⁴ $(k_x + ik_y)\hat{e}_z$ corresponding to the same time reversal broken pairing state as ^3He-A . We also found that at much lower temperatures, additional transitions occurred where the f wave and p_z order parameters become non-zero. The gap function has line nodes on the Fermi surface, in agreement with experiment, only when the f wave component is zero. Arguing that the f wave component would be suppressed by impurities, we showed that with the f wave component removed, one obtains excellent agreement between the calculated and experimental specific heat, penetration depth and thermal conductivity. We show, in Sec. IV below, that this removal of the f wave component is justified by the presence of weak disorder.

It is important to ask how these results depend on the details of the assumptions made in the model. In order to test the stability of our results to variations in the model we therefore introduced some additional subdominant interaction parameters. For our initial exploration of the issues involved we have generalized Eqs. (20) and (21) as follows:

$$U_{km}^0 = \begin{pmatrix} 0 & u & u & u \\ u & u & u & u \\ u & u & u & u \\ u & u & u & U_k \end{pmatrix} A \quad (22)$$

$$U_{mm}^0 = \begin{pmatrix} 0 & U_? & U_? & u^0 \\ U_? & U_? & U_? & u^0 \\ u^0 & u^0 & u^0 & u^0 \end{pmatrix} A ;$$

Reassuringly, with these modified parameters we obtained a temperature dependence of the gap parameters which are qualitatively similar to those for the original parameters. It is interesting to note that for fixed values of $U_?$ and U_k the changes of u and u^0 hardly change the superconducting transition temperature. We have systematically studied the effect of additional interactions, especially so on the line $u = u^0$, and found small differences compared to the $u = 0$ solution even for u as large as $0.28t$. The differences are mainly connected with the appearance of out of plane components of j_{cc}^{\perp} generated by the new interactions as is evident from Fig.(3). For larger values of u the difference becomes more significant (Fig. 3a). Note, however, that only low temperature dependence of the pairing amplitudes is affected. In Fig. 3b we show the variation of a few characteristic j_{mm} against u at zero temperature. Clearly, for $u > 0.3t$ there is a qualitative change of our solution leading to dominant out of plane pairing components in all orbitals. Large u also affects the critical temperature T_c . Interestingly, for finite u we also observe increasing values of in-plane pairing amplitudes in the a and b channels: $j_{mm}^{\perp p_x}$ and $j_{mm}^{\perp p_y}$ for $m^0 = a; b$. Reassuringly, the corresponding specific heat (Fig. 4) is essentially unchanged and remains in equally good agreement with the experiments. Therefore we conclude that the solution we have found is not very specific to the precise details of the model parameters which we assumed, but is a generic solution valid for at least some range of the possible interaction parameters of the form depicted in Eq. 22.

The quasiparticle energy gap structure which we obtained is shown in Fig. 5. The gap is finite everywhere on the sheet, Fig. 5(d), although it is very anisotropic, and becomes small when the Fermi surface approaches near to the van Hove points at $(\pi; 0)$ and $(0; \pi)$. In contrast, the a and b Fermi surface sheets have gap zeros in the vicinity of the lines $k_z = \pm c$. In the case of the

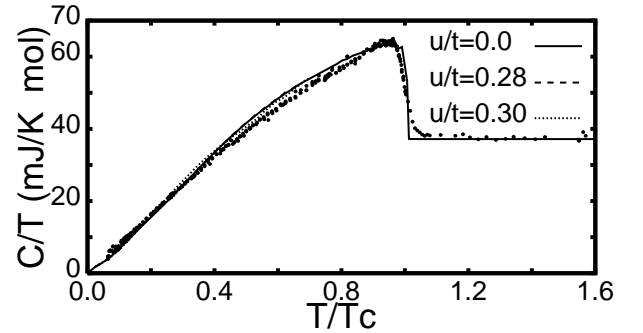


FIG. 4: Calculated specific heat for a three parameters u ($= u^0$) ($u/t = 0.0$; 0.28 and 0.30 corresponding to full dashed and dotted lines, respectively) compared to the experimental data (points) of Nishizaki et al.[8]

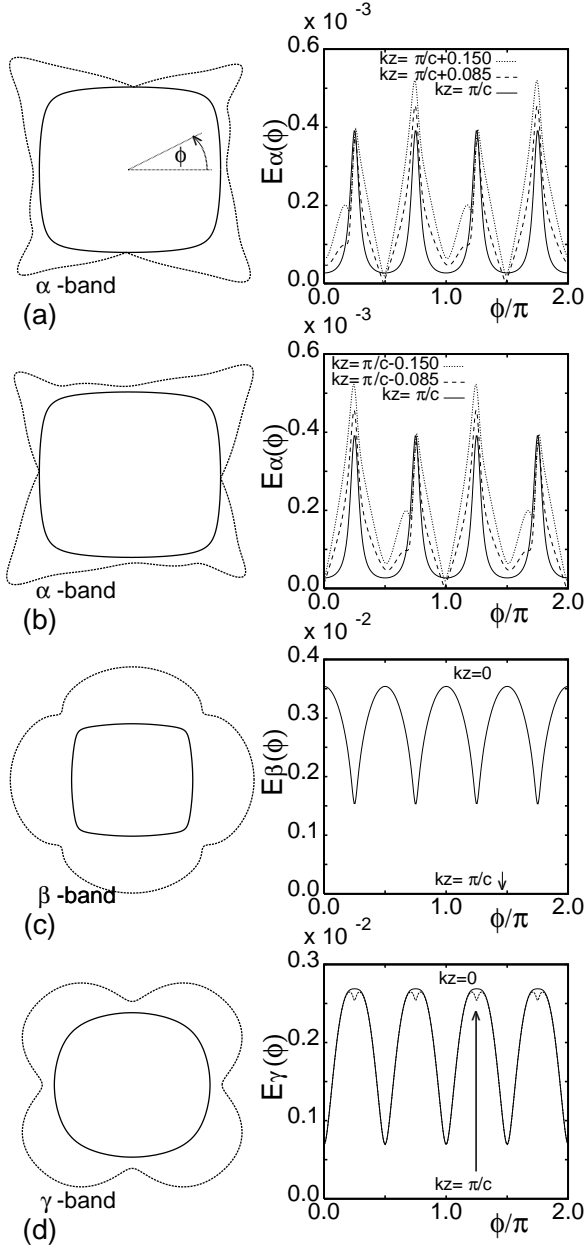


FIG. 5: Lowest energy eigenvalues, $E(k)$ on the Fermi surface; sheet in the plane $k_z = c + 0.085$ (a) and $k_z = c + 0.085$ (b), (c) and (d) sheets in the plane $k_z = 0$.

gap is zero to numerical accuracy on these nodal lines. While in the case of the gap is very small on these lines, but not exactly zero. In fact there are eight point nodes on the sheet, as can be seen in Fig. 5 (a,b). Two point nodes lie just above the $k_z = c$ line at $k_z = c + 0.085$ at two different angles. Another pair lie just below, at $k_z = c - 0.085$ at an angle rotated by $\phi = \pi/2$. The remaining four are located in similar positions near the

line $k_z = c$. This interesting nodal structure arises from the fact that the Fermi surface cylinder is centered at X in the Brillouin zone not at Γ (Fig. 2), and therefore it has two-fold symmetry not four fold like Γ . Notice also that the excitation gap on the sheet is non-zero even when $a_a = a_b = b_b = 0$, because it is hybridized to the c orbital and $c \notin 0$.

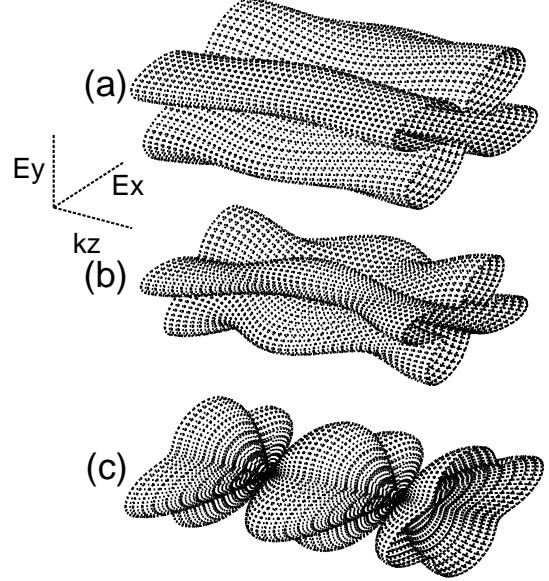


FIG. 6: Minimum energy quasiparticle eigenvalues on the Fermi surface sheet, $E(k_F)$, plotted in cylindrical polar coordinates as functions of k_z and a b plane polar angle, ϕ . Parameter values are $u=t=0.28$ (a), 0.30 (b), 0.32 (c), respectively. One can see that for $u=0.3$ the sheet gap is nodeless, while for $u>0.3$ line nodes appear at $k_z = c$.

Note that this nodal structure of the gap is unchanged by the presence of the small subdominant interaction parameter u , in Eq.(22). However, upon increasing the value of the u parameter eventually the results change qualitatively, leading to appearance of additional line nodes in (Fig. 6) for $u=0.32t$. In this case the band gap also develops a line node, similar to the behavior of the band.

IV. EFFECTS OF DISORDER

As we noted it earlier, to obtain agreement with experiment we had to eliminate the f-wave component $\chi_{mm}^f(T)$ and we suggested that this can be done by an appeal to the effects of a small amount of disorder. We shall now substantiate this contention by explicit calculations.

In case of non-magnetic disorder our Hamiltonian can

V. BOND-PROXIMITY EFFECTS

To get a single superconducting transition temperatures within our interlayer coupling model we are forced to tune two interaction parameters. However, it has been proposed²⁵ that a single transition can be obtained in a multiband model by allowing for a symmetry mixing interaction of the type $U(\mathbf{k}; \mathbf{q}) = g^0 f(\mathbf{k})g(\mathbf{q})$, where $f(\mathbf{k})$ and $g(\mathbf{q})$ are order parameter symmetry functions for respective bands.

It is the aim of the present section to check to which extent similar approach may be used in our bond model. We start with short discussion of the source and magnitude of symmetry mixing interaction. The description we have used is a real space, two point near neighbour interaction such as naturally arises in any multi-orbital, extended, negative U Hubbard model, Eq. 12. To be quite clear about this matter we recall that a generic pair-wise interaction like $U(\mathbf{r}; \mathbf{r}')$, when expressed in the language of a tight-binding model Hamiltonian will, in general, give rise to four point interaction parameters U_{ijkl} . The original Hubbard Hamiltonian makes use of the one point parameters $U_i^{(1)} = U_{ii,ii}$ whilst the extended Hubbard model is based on two point parameters $U_{ij,jl}^{(2)} = U_{ij,jl}$. Evidently our bond model is a negative U -version of the latter³⁷. The symmetry mixing interactions²⁵ arise from 3-site interactions $U_{ij,jl}^{(3)}$. The physics of this is often referred to as assisted hopping³⁸. If one assumes, as is normally the case in an isotropic substance, that $j^{(1)}j > j^{(2)}j > j^{(3)}j > j^{(4)}j$ then the bonds represent stronger coupling than assisted hopping and should be the preferred coupling mechanism. However, for the tetragonal arrangement of Ru atoms in Sr_2RuO_4 this is no more than a suggestion at present.

In the presence of a three point interaction $U_{ij,jl}^{(3)} = U_{ij,jl} = U_I$, for all nearest neighbours ijl such that i and j are in one Ru plane while l is on a neighbouring one (Fig. 1), the gap equation (Eqs. 16-18) can be rewritten in k -space as,³⁹

$$\begin{aligned} m_{m^0}^0(\mathbf{k}) = & \frac{1}{N} \sum_{\mathbf{q}} U_{m_{m^0}^0}^0(\mathbf{k}-\mathbf{q}) m_{m^0}^0(\mathbf{q}) \\ & + \frac{1}{N} \sum_{\mathbf{q}; \text{oo}^0} U_{m_{m^0}^0; \text{oo}^0}^0(\mathbf{q}; \mathbf{k}-\mathbf{q}) o_{\text{oo}^0}^0(\mathbf{q}) : (29) \end{aligned}$$

where, as before,

$$m_{m^0}^0(\mathbf{k}) = u_{\mathbf{k}m} v_{\mathbf{k}m^0} (1 - 2f(E)) : (30)$$

In a body centered tetragonal crystal (Fig. 1) the various matrix elements of the general four point interaction $U_{m_{m^0}^0; \text{oo}^0}$ responsible for p-wave pairing can be written (suppressing spin indices for clarity):

$$U_{cc}(\mathbf{k}; \mathbf{q}) = 2U_I V(\mathbf{k})V(\mathbf{q}) \quad (31)$$

$$U_{m_{m^0}^0}(\mathbf{k}; \mathbf{q}) = 8U_I \nabla(\mathbf{k})\nabla(\mathbf{q}) \quad \text{for } m; m^0 = a; b$$

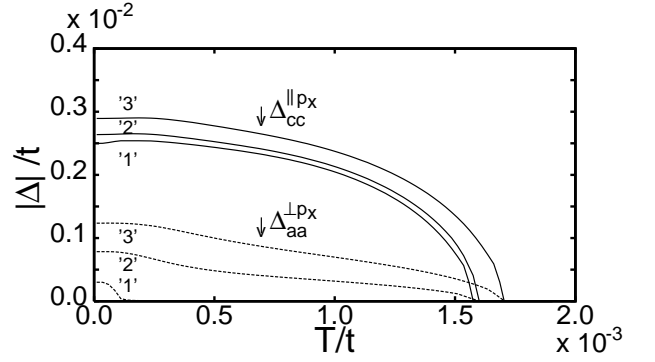


FIG. 9: Order parameters $j_{cc}^{p_x}$, $j_{aa}^{p_x}$ for $U_I = 0.400t$, $U_K = 0.494t$ and the proximity coupling as functions of temperature. The three curves '1', '2' and '3' correspond to the values 0.0, 0.005, 0.010 of three point coupling constant.

$$U_{m_{m^0}; cc}(\mathbf{k}; \mathbf{q}) = 8U_I V(\mathbf{k})V(\mathbf{q}) \quad \text{for } m^0; m = a; b$$

$$U_{cc; m^0}(\mathbf{k}; \mathbf{q}) = 8U_I V(\mathbf{k})V(\mathbf{q}) \quad \text{for } m^0; m = a; b$$

where $V(\mathbf{k})$ and $\nabla(\mathbf{k})$ are respectively:

$$V(\mathbf{k}) = (\sin k_x + \sin k_y) \quad (32)$$

$$\nabla(\mathbf{k}) = \sin \frac{k_x}{2} \cos \frac{k_y}{2} + \sin \frac{k_y}{2} \cos \frac{k_x}{2} \cos \frac{k_z c}{2} :$$

Note that the three point interaction leads to an extra interlayer coupling proportional to U_I . Interestingly, the general form of the order parameter is the same as previously derived (Eqs. (16-19)) despite the additional three point coupling Eq. (32) in the self-consistency relation Eqs. (30-31).

It has to be noted that the presence of interaction U_I strongly changes T_c . To get its correct value (1.5K) for the present model we have taken $U_I = 32\text{meV}$ and $U_K = 40\text{meV}$ and repeated our calculations for various U_I values. The results are shown in Figs. (9) and (10).

Fig. (9) shows the results for the amplitudes $j_{cc}^{p_x}(T)$ and $j_{aa}^{p_x}(T)$ including the three-point interaction. Note that for $U_I = 0$ (curves labeled by (1) in the figure) the

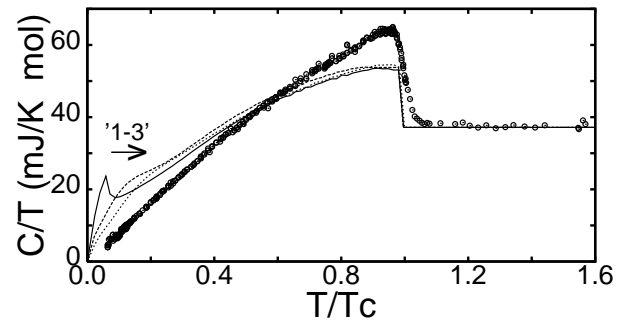


FIG. 10: Specific heat and the effect three point interaction, compared to the experimental data of Nishizaki et al. [8]. The arrow indicates increasing values of the proximity coupling ('1-2-3' as in Fig. 9).

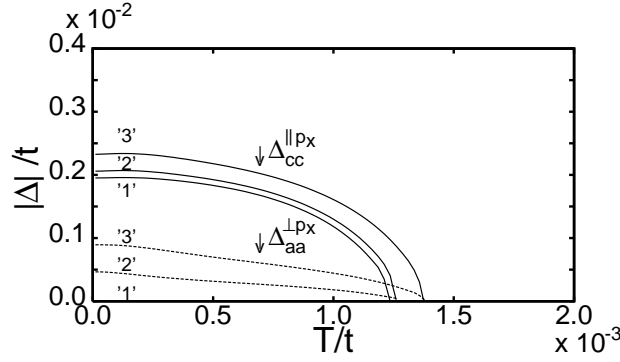


FIG. 11: Order parameters $\Delta_{aa}^{p_x}$, $\Delta_{cc}^{p_x}$ for $U_z = 0.400t$, $U_k = 0.494t$ and the proximity coupling as functions of temperature in disordered system $U_I = 0.005t$. The three curves '1', '2' and '3' correspond to the values $U_I = 0.0, 0.005, 0.010$ of three point coupling constant.

temperature where $\Delta_{cc}^{p_x}(T)$ becomes non-zero is much higher than that where $\Delta_{aa}^{p_x}(T)$ becomes non-zero. It is evident from the figure that for $U_I \neq 0$ the parameters $\Delta_{m0}(T)$ for a, b and c orbitals vanish at the same temperature and two transitions merge into one. Thus, the proximity coupling mechanism identified by ZR²⁵ in their band description of the electron-electron interaction, also works in our bond model.

Intriguingly, although the proximity coupling works in principle, the above mechanism does not seem to be helpful in the context of building phenomenological interactions suitable to describe experimental data. To illustrate this point we reproduce, in Fig. (10), the specific heat corresponding to the set of $\Delta_{cc}^{p_x}(T)$ and $\Delta_{aa}^{p_x}(T)$ shown in Fig. (9). Clearly, as U_I increases the second transition at low temperature becomes enlarged and merges with the first transition at higher temperature. However, the small values of U_I shown in Figs. (9, 10) are not sufficient to get the specific heat jump at T_c right. Therefore U_I must be large for the ZR scenario to fit the experiments. By contrast, as we have demonstrated earlier, if $U_I = 0$ and the sizes of U_z and U_k are adjusted so that only one transition occurs both the low temperature slope and the jump at T_c agrees with experiments. Thus although we have not investigated models featuring a 'proximity effect' induced by $U^{(3)}$ type of interactions systematically we conclude that such interactions are not needed to fit the available data.

Finally, it is also interesting to see what are the effects of disorder on the 'orbital proximity effect'; the results are shown in Fig. 11. We see that, disorder can eliminate the gap on π sheets, while leaving it almost unchanged on σ sheets. This feature of the proximity effect scenario opens it up for experimental verification by measurement on samples with increasing disorder. Evidently the effect of disorder should be that the low temperature power laws disappear due to the destruction of superconductivity on the π sheets.

V I. C onclusions

We have introduced a methodology for building semi-phenomenological, attractive electron-electron interactions bond by bond for calculating superconducting properties under circumstances when the physical mechanism of pairing is not known. We deployed it to study p-wave pairing in Sr_2RuO_4 . A bond was described by an interaction constant $U_{m0}(ij)$ which depends on the sites i and j , the orbitals m and m' , and their spin orientation and σ . We have solved the appropriate Bogoliubov de Gennes equations for a number of scenarios defined by a small set of interaction constants. We have found that the one for which $U_{cc}^{p_x}(ij) = U_z$ for i and j being nearest neighbour Ruthenium atoms in the Ru-O planes and $U_{aa}^{p_x}(ij) = U_{bb}^{p_x}(ij) = U_z$ for i and j being nearest on neighbouring planes explained most of the available experimental data. Namely, the corresponding solution featured a gap function on the π -sheet of the form $\Delta_{cc}(k) = \sin k_x + i \sin k_y$ and a line of gap on the σ sheet. For this scenario the requirement that there be only one transition at $T_c \approx 1.5$ K fixed both U_z and U_k and hence all further results could be regarded as quantitative predictions of the model. Remarkably, the model gave a satisfactory account of the data for the specific heat $C(T)$, superfluid density $n_s(T)$ and the thermal conductivity $\kappa(T)$.

We have also investigated the stability of the model to introduction of further interaction constants and disorder. We found that the predictions of the model are robust to changes of new interactions, while disorder mainly affects the f-wave solution. Thus we can conclude that the experimental data support a simple model which describes, quantitatively, the p-wave pairing observed in Sr_2RuO_4 on the basis of two orbital specific coupling constants: $U_k = 40$ meV, $U_z = 48$ meV. The central physical feature of the model is that U_k corresponds to interaction between electrons in the Ruthenium planes while U_z describes an inter-plane interaction of roughly equal strength.

In view of the above results, we would like to emphasize two points. Firstly, we have proposed an alternative to the 'intra-band proximity effect' model of Zhitomirsky and Rice²⁵ for describing horizontal line nodes on the π sheets of the Fermi Surface in superconducting Sr_2RuO_4 . Our bond model differs from theirs in the way the interlayer coupling is implemented. The extension of the model in the spirit of ZR has also been studied by allowing for 3-site interactions in the Hamiltonian. Even though the resulting 'bond proximity model' features single superconducting transition temperature the original model with fine-tuned two interactions gives better fit to experimental T dependence of the specific heat.

Acknowledgments

This work has been partially supported by KBN grant No. 2P 03B 106 18, the Royal Society Joint Project and

the NATO Collaborative Linkage Grant 979446. We are grateful to Prof. Y. Maeno for providing us with the experimental specific heat data reproduced in Figs. 4 and 10.

-
- ¹ Y. Maeno, T. M. Rice and M. Sigrist, *Physics Today* 54, 42 (2001).
 - ² A. P. Mackenzie, Y. Maeno, *Rev. Mod. Phys.*, 75 657 (2003).
 - ³ A. J. Leggett, *Rev. Mod. Phys.*, 47 331 (1975).
 - ⁴ A. Mackenzie and Y. Maeno, *Physica B* 280, 148 (2000).
 - ⁵ C. Bergemann, S. R. Julian, A. P. Mackenzie, S. Nishizaki and Y. Maeno, *Phys. Rev. Lett.* 84 2662 (2000).
 - ⁶ T. M. Rice and M. Sigrist, *J. Phys.: Condens. Matter* 7, L643-L648 (1995).
 - ⁷ K. Ishida et al., *Nature* 396, 658 (1998).
 - ⁸ J. A. Du y et al., *Phys. Rev. Lett.* 85 5412 (2000).
 - ⁹ S. Nishizaki, Y. Maeno and Z. Mao, *J. Phys. Japan* 69, 336 (2000).
 - ¹⁰ I. Bonalde et al., *Phys. Rev. Lett.* 85, 4775 (2000).
 - ¹¹ K. Izawa et al., *Phys. Rev. Lett.* 86, 2653 (2001).
 - ¹² G. M. Luke et al. *Nature* 394 558 (1998).
 - ¹³ G. E. Volovik and L. P. Gor'kov, *Zh. eksp. teor. Fiz.* 88, 1412 (1985) [*Sov. Phys. JETP*, 61, 843 (1985)].
 - ¹⁴ M. Ozaki, K. Machida and T. Ohm i, *Prog. Theor. Phys.* 75, 422 (1986).
 - ¹⁵ M. Sigrist and T. M. Rice, *Z. Phys. B* 68, 9 (1987).
 - ¹⁶ M. Ozaki and K. Machida, *Phys. Rev. B* 39, 4145 (1989).
 - ¹⁷ J. F. Annett, *Adv. Phys.* 39, 83 (1990).
 - ¹⁸ M. Sigrist and K. Ueda, *Rev. Mod. Phys.* 63, 239 (1991).
 - ¹⁹ M. J. Graf and A. V. Balatsky, *Phys. Rev. B* 62, 9697 (2000).
 - ²⁰ H. W on and K. Maki, *Europhys. Lett.* 52, 427-433 (2000).
 - ²¹ T. Dahm, H. W on, and K. Maki, cond-mat/0006301.
 - ²² I. Eremin, D. Manske, C. Koas and K. H. Bennemann, cond-mat/01020774.
 - ²³ D. Manske, I. Eremin and K. H. Bennemann, in *New Trends in Superconductivity*, J. F. Annett and S. Kuchinin (eds.) 293-305, (Kluwer, 2002).
 - ²⁴ D. F. Agterberg, T. M. Rice and M. Sigrist, *Phys. Rev. Lett.* 73 3374 (1997).
 - ²⁵ M. E. Zhitomirsky and T. M. Rice, *Phys. Rev. Lett.* 87, 057001 (2001).
 - ²⁶ J. F. Annett, G. Litak, B. L. Gyor y and K. I. Wysokinski, *Phys. Rev. B* 66, 134514 (2002).
 - ²⁷ Y. Hasegawa, K. Machida and M. Ozaki, *J. Phys. Japan* 69, 336 (2000).
 - ²⁸ A. P. Mackenzie et al., *Phys. Rev. Lett.* 76, 3786 (1996). Note the corrected Fermi surface parameters in: Y. Maeno et al., *J. Phys. Soc. Japan* 66, 1405 (1997).
 - ²⁹ Z. Szotek, B. L. Gyor y, W. M. Temmerman, O. K. Andersen, O. Jepsen, *J. Phys. Condens. Mat.* 13, 8625 (2001).
 - ³⁰ K. Miyake and D. Narikiyo, *Phys. Rev. Lett.* 83 1423 (1999).
 - ³¹ A. M. Martin, G. Litak, B. L. Gyor y, J. F. Annett and K. I. Wysokinski, *Phys. Rev. B* 60 7523 (1999).
 - ³² G. Litak, J. F. Annett, B. L. Gyor y, *Acta Phys. Pol. A* 97, 249 (2000).
 - ³³ G. Litak, J. F. Annett, B. L. Gyor y, in *Open Problems in Strongly Correlated Electron Systems* Ed. J. Bonca et al. (Kluwer Academic Publishers NATO Science Series, Dordrecht 2001) pp. 425(427).
 - ³⁴ G. Litak, *Phys. Stat. Sol. B* 229, 1427 (2002).
 - ³⁵ D. F. Agterberg, *Phys. Rev. B* 60 R 749 (1999).
 - ³⁶ E. R. Hansen, *A Table of Series and Products*, (Prentice Hall, Inc., Englewood Cliffs, N. J. 1975).
 - ³⁷ R. M. McNas et al., *Rev. Mod. Phys.* 62, 113 (1991).
 - ³⁸ D. L. Cox and A. Zawadowski, *Exotic Kondo Effects in Metals*, (Taylor and Francis, London 1999).
 - ³⁹ G. Litak, J. F. Annett, B. L. Gyor y and K. I. Wysokinski, in *New Trends in Superconductivity* Eds. J. F. Annett and S. Kuchinin (Kluwer Academic Publishers, Dordrecht 2002) pp. 307(316).
 - ⁴⁰ K. I. Wysokinski, G. Litak, J. F. Annett, B. L. Gyor y, *Phys. Stat. Sol. B* 236 325 (2003).